J. Cent. South Univ. (2015) 22: 1892−1900
DOI: 10.1007/s11771-015-2708-2

Springer

Coupled hydro-mechanical analysis of slope under rainfall using modified elasto-plastic model for unsaturated soils

WANG Liu-jiang(王柳江)[1], LIU Si-hong(刘斯宏)[1], FU Zhong-zhi(傅中志)[2], LI Zhuo(李卓)[2]

1. College of Water Conservancy and Hydropower Engineering, Hohai University, Nanjing 210098, China;
2. Nanjing Hydraulic Research Institute, Nanjing 210029, China

Abstract: Two modifications for the basic Barcelona model (BBM) are present. One is the replacement of the net stress by the average skeleton stress in unsaturated soil modeling, and the other is the adoption of an expression for the load−collapse (LC) yield surface that can match flexibly the normal compression lines at different suctions. The predictions of the modified BBM for the controlled-suction triaxial test on the unsaturated compacted clay are presented and compared with the experimental results. A good agreement between the predicted and experimental results demonstrates the reasonability of the modified BBM. On this basis, the coupled processes of groundwater flow and soil deformation in a homogeneous soil slope under a long heavy rainfall are simulated with the proposed elasto-plastic model. The numerical results reveal that the failure of a slope under rainfall infiltration is due to both the reduction of soil suction and the significant rise in groundwater table. The evolution of the displacements is greatly related to the change of suction. The maximum collapse deformation happens near the surface of slope where infiltrated rainwater can quickly reach. The results may provide a helpful reference for hazard assessment and control of rainfall-induced landslides.

Key words: unsaturated soils; modified basic Barcelona model (BBM); numerical analysis; rainfall infiltration; model slope

1 Introduction

Unsaturated soil exists widely in geotechnical engineering such as compacted fills and natural soils above the water table. Given the fact that unsaturated soils can experience significant volumetric and mechanical changes during the change of degree of saturation, which often leads to engineering problems such as the damage of foundation and slope failure under rainfall infiltration [1−2], the deformation analysis for unsaturated soils is thus necessary in practice. As a result, this is a coupled hydro-mechanical problem and the understanding of the coupled hydro-mechanical behavior of unsaturated soils is important in the geotechnical analysis or design. Various formulations have been presented [3−6]. The discussion indicates that two key problems need to be solved for the deformation analysis of unsaturated soils. One is the mechanical constitutive model adopted for the unsaturated soils which is of profound importance in a coupled hydro-mechanical problem. The other is the applicable implement of unsaturated soil models in the finite element method in engineering.

Elasto-plastic constitutive modeling for unsaturated soils was pioneered by the work of ALONSO et al [7], which led to the complete formulation of an elasto-plastic model. This model, known as the basic Barcelona model (BBM), uses the net stress and suction as the stress variables and introduces a load−collapse (LC) yield surface that defines the variation of the apparent preconsolidation stress with the suction. It is capable of reflecting some basic features of unsaturated soils, including the elasto-plastic volume decrease (collapse) during wetting or isotropic compression, the change of stiffness and shear strength with the suction, and the moderate volume increase during wetting. Since then, following the same framework as ALONSO et al [7], a large number of constitutive models for unsaturated soils have been proposed [8−10]. In recent years, researchers have mainly focused on incorporating suction−saturation relationships by integrating hysteresis into stress−strain relationship [11−14].

Despite the existence of a number of models, the suction is always considered as an additional stress variable in different models. However, there is little consensus on whether an independent stress (e.g. net stress or total stress) or stress variable such as Bishop's effective stress should be used. From the discussion by SHENG et al [15], the early model such as the BBM that

Foundation item: Project(1301015A) supported by the Post-doctoral Research Fund of Jiangsu Province, China; Project Funded by the Priority Academic Program of Jiangsu Higher Education Institution, China; Project(2014M561566) supported by China Postdoctoral Science Foundation; Project(YK913007) supported by Key Laboratory of Earth-Rock Dam Failure Mechanism and Safety Control Technologies, China
Received date: 2014−04−04; **Accepted date:** 2014−09−05
Corresponding author: LIU Si-hong, PhD; Tel: +86−25−83786727; E-mail: sihongliu@hhu.edu.cn

uses net stress and suction as stress variables has a major problem of the discontinuity at the transition between saturated and unsaturated state. This is because stress variables used for unsaturated state (total stress) do not turn into the stress variables for saturated state (effective stress). Besides, in the original presentation of the BBM, the compression lines for different suction values were assumed to diverge with increasing applied stress, so that the potential for wetting-induced collapse compression increased with the stress level. However, the experimental evidence shows the opposite behavior for some unsaturated soils, and this has often been taken as a limitation on the applicability of the BBM. Moreover, the initial mean stress of the unsaturated soils often exceeds a critical value p (corresponding to the maximum collapse during wetting) in most of practical geotechnical engineering. To overcome the above shortcomings and describe the hydraulic and mechanical behavior of unsaturated soils properly, an alternative expression for LC yield surface and the Bishop typed stress-state variables need to be proposed.

Therefore, the main objective of this work is the presentation of two modifications for the BBM. One is the replacement of the net stress with the average skeleton stress in unsaturated soil modeling, and the other is the adoption of an alternative expression for the LC yield surface that can match flexibly the normal compression lines at different suctions. The modified BBM will then be verified through the comparison between predictions and experimental data from the suction-controlled triaxial tests on the unsaturated compacted clay. The second part of the work outlines the gradients for implementing unsaturated soil models into the finite element method. Finally, the modified BBM is applied in a numerical analysis by modeling a slope under the infiltration of rainfall to demonstrate the reasonability of the modified BBM in the deformation analysis of the unsaturated soils.

2 Basic Barcelona model

The well-known basic Barcelona model (BBM) was first presented by ALONSO et al [7] and then widely adopted as a framework of other elasto-plastic constitutive models for unsaturated soils. It can describe not only the swell-shrink characteristics of unsaturated soils under wetting−drying cycles, but also the collapse caused by the decrease in suction and the isotropic compression. The elastic volumetric strain increment and the elastic shear strain increment in the BBM can be given as

$$\mathrm{d}\varepsilon_{\mathrm{v}}^{\mathrm{e}}=\frac{\kappa}{v}\frac{\mathrm{d}p}{p}+\frac{\kappa_{\mathrm{s}}}{v}\frac{\mathrm{d}s}{s+p_{\mathrm{at}}} \tag{1}$$

$$\mathrm{d}\varepsilon_{\mathrm{s}}^{\mathrm{e}}=\frac{1}{3G}\mathrm{d}q \tag{2}$$

where $v(=1+e)$ is the specific volume; κ and κ_{s} are the elastic stiffness parameters related to the changes in net mean stress and suction, respectively; p is the net mean stress, q the deviator stress, p_{at} the atmospheric pressure and G the shear modulus.

In the BBM, the yield function f and the plastic potential g are defined in terms of the net mean stress, the suction and a hardening parameter. There are two yield surfaces of the load−collapse (LC) and the suction increase (SI) in a generalized stress space. By adopting the associated flow rule, the yield function f and plastic potential g for the LC yield surface and for the SI yield surface are respectively expressed as

$$f^{\mathrm{LC}}=g^{\mathrm{LC}}=q^2-M^2\left(p+p_{\mathrm{s}}\right)\left(p_0-p\right)=0 \tag{3}$$

$$f^{\mathrm{SI}}=g^{\mathrm{SI}}=s-s_0=0 \tag{4}$$

where M is the slope of the critical state lines, p_0 is the pre-consolidation pressure, p_{s} is the cohesion associated with suction, and s_0 is a hardening parameter controlling the suction increase in the yield curve. Figure 1 shows the shape of the yield surfaces in the p-q-s space.

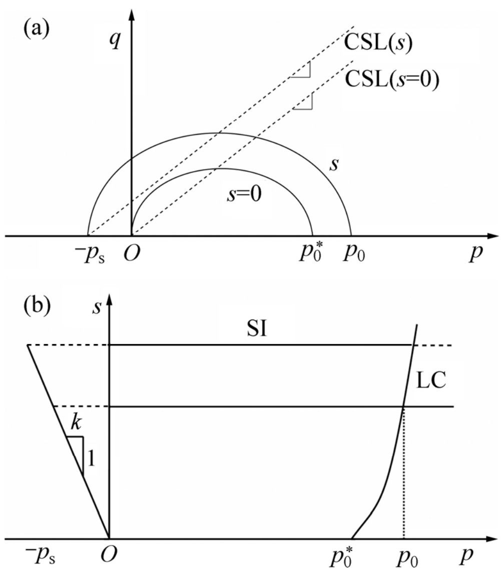

Fig. 1 Yield surfaces of BMM in p-q-s space: (a) Yield surface in p-q plane; (b) Yield surface in p-s plane

The core of the BBM is the load−collapse (LC) yield surface, which defines the variation of the apparent preconsolidation stress with the soil suction. In the BBM, the LC yield surface is characterized as

$$p_0=p^{\mathrm{c}}\left(\frac{p_0^*}{p^{\mathrm{c}}}\right)^{\frac{\lambda(0)-\kappa}{\lambda(s)-\kappa}} \tag{5}$$

where p^{c} is a reference stress; p_0^* is the preconsolidation net mean stress under a saturated condition, which is also regarded as a hardening parameter for the LC yield surface; $\lambda(0)$ and $\lambda(s)$ are the slopes of the normal compression line (e−ln$p$) under the saturated and the unsaturated states along the virgin isotropic loading, respectively. As the soil stiffness increases with suction, $\lambda(s)$ is assumed to be

$$\lambda(s)=\lambda(0)\left[(1-r)\mathrm{e}^{-\beta s}+r\right] \tag{6}$$

where r is a constant associated with the maximum stiffness of the soil; β is a parameter that controls the increase of the soil stiffness with the suction.

3 Stress-state variables for unsaturated soils

The net stress and suction are used as the stress-state variables in the BBM, which can turn discontinuous during the transition between saturated and unsaturated states since the total stress variables for an unsaturated state cannot change into the effective stress variables for a saturated state. In order to identify properly and describe continuously the hydraulic and mechanical behavior of an unsaturated soil, the average stress tensor which is used as the stress variables in this work, is defined as

$$\sigma'_{ij}=\sigma_{ij}-u_{\mathrm{a}}\delta_{ij}+S_{\mathrm{r}}s\delta_{ij} \tag{7}$$

where σ_{ij} is the total stress, u_{a} the pore-air pressure, δ_{ij} the Kronecker delta, S_{r} the degree of saturation and s the suction (s=u_{a}−u_{w}).

As the pore-air pressure remains a constant, usually equal to the atmospheric pressure for many geotechnical problems, it is not treated as a variable. Thus, the suction is replaced with a negative pore-water pressure with respect to the atmospheric pressure. Ignoring the pore-air pressure, Eq. (7) is rewritten as

$$\sigma'_{ij}=\sigma_{ij}-S_{\mathrm{r}}u_{\mathrm{w}}\delta_{ij} \tag{8}$$

where u_{w} is the pore-water pressure. The average stress tensor defined in Eq. (8) permits a smooth transition between the saturated and unsaturated states.

4 Modification for BBM

ALONSO et al [7] assumed that the normal compression lines for different suctions would diverge when the applied stress increases, so that the plastic potential for wetting induced collapse compression would increase with the stress level. However, many experimental evidences give the opposite results for some unsaturated soils. This has been regarded as a limitation of the BBM. YUDHBIR's study [16] showed that the wetting induced collapse compression initially increases with mean stress p and subsequently decreases with stress level at a higher p value. JOSA et al [17] proposed an elasto-plastic model for unsaturated soils by modifying $\lambda(s)$, and the experiments on the compacted speswhite kaolin clay performed by WHEELER and SIVAKUMAR [8] showed that $\lambda(s)$ increases with suction. To describe this property, the following formulation for $\lambda(s)$ as proposed by SUN et al [13] is used in this work:

$$\lambda(s)=\lambda(0)+\frac{\lambda_{\mathrm{s}}s}{p_{\mathrm{at}}+s} \tag{9}$$

where λ_{s} is a soil parameter. When suction tends to infinity, the slope of the virgin normal compression line approaches $\lambda(0)$+λ_{s}, as illustrated in Fig. 2. Therefore, the wetting induced collapse won't increase infinitely with mean stress.

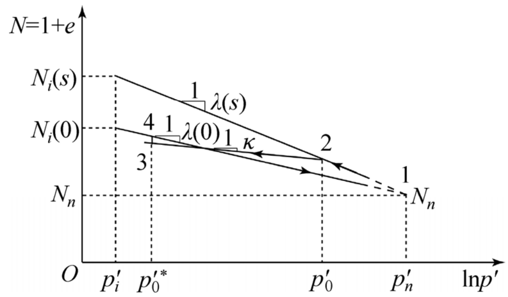

Fig. 2 Compression curve for saturated and unsaturated soil

In the BBM, it is also assumed that there exists a pressure p^{c} at which the LC yield curve is a vertical straight line, but it is not clear how to identify it for a particular soil from the laboratory test data. As pointed out by many researchers, it is extremely difficult and inaccurate to identify the value of p^{c} from the experimental data, as direct information on how the yield curve shape develops is rarely available. Thus, WHEELER and SIVAKUMAR [8] proposed a relatively complex mathematic expression for the LC yield surface to match flexibly the normal compression lines at different suctions:

$$\left(\lambda(s)-\kappa\right)\ln\frac{p_0}{p_{\mathrm{at}}}=\left(\lambda(0)-\kappa\right)\ln\frac{p_0^*}{p_{\mathrm{at}}}+N(s)-N(0)+\kappa_{\mathrm{s}}\ln\frac{s+p_{\mathrm{at}}}{p_{\mathrm{at}}} \tag{10}$$

where $N(s)$ and $\lambda(s)$ are the intercept and the slope of the normal compression line at a given suction s, respectively; $N(0)$ and $\lambda(0)$ are the corresponding values at zero suction. The advantage of this approach over that presented by ALONSO et al [7] is that the experimental measurement of $N(s)$ at a few different suction values is more feasible than identifying the value of the reference pressure p^{c}.

Many experiments indicate that the normal compression lines at different values of suction in the larger range of isotropic stress will converge at one point in e−ln p' plane (Fig. 2), at which the variations of suction will not induce any plastic volumetric strain.

Consider the response of two samples to isotropic loading at different suctions: s=0 (saturated case) and s>0 (unsaturated case), as shown in Fig. 2. The two normal compression lines converge at the Point 1 (p'_n, N_n). These two samples have the preconsolidation stresses of $p_0'^*$ (Point 4 in Fig. 2) and p'_0 (Point 2 in Fig. 2), respectively. If both Point 2 and Point 4 in Fig. 2 belong to the same yield curve in s-p space, the change of the specific volumes through the path 1-2-3-4 for the unsaturated sample is the same as that through the unloading path 1-4 for the saturated sample. The swelling induced by the suction reduction from Point 3 to Point 4 in the elastic domain is assumed to be

$$N(s)-N(0)=-\kappa_{\mathrm{vs}}\ln\left(s+p_0'^*\right) \tag{11}$$

where the slope κ_{vs} is identical to the slope κ_{vp} when the suction is zero and then gradually decreases to zero as suction turns positive. A simple approximation would be of the following form:

$$\kappa_{\mathrm{vs}}=\frac{\kappa_{\mathrm{vp}}}{s+1} \tag{12}$$

Taking Eq. (11) into account, a relationship between p'_0 and $p_0'^*$ could be obtained by relating the change of the specific volumes through the path 1-2-3-4 to the path 1-4:

$$N_n+\lambda(s)\ln\frac{p'_n}{p'_0}+\kappa\ln\frac{p'_0}{p_0'^*}+\kappa_{\mathrm{vs}}\ln\left(s+p_0'^*\right)=N_n+\lambda(0)\ln\frac{p'_n}{p_0'^*} \tag{13}$$

From Eq. (12) and Eq. (13), an alternative equation for the LC yield surface is rewritten as

$$p'_0=p'_n\left(s+p_0'^*\right)^{\frac{\kappa_{\mathrm{vp}}}{(\lambda(s)-\kappa)(s+1)}}\left(\frac{p_0'^*}{p'_n}\right)^{\frac{\lambda(0)-\kappa}{\lambda(s)-\kappa}} \tag{14}$$

In this work, the BBM is modified by taking into account the stress-state variables of Eq. (8), the normal compression line with a slope of Eq. (9) and the equation (13) for the LC yield surface. In this modified model, the reference stress p^{c} is replaced by p'_n, which is easier to determine from experimental data.

5 Formulation of modified BBM in general stress

In the modified BBM, the yield function is written as

$$f=q^2-M^2(p'+p'_{\mathrm{s}})(p'_0-p')=0 \tag{15}$$

The associated flow rule is followed in terms of the average skeleton stress space:

$$\mathrm{d}\varepsilon_{ij}^{\mathrm{p}}=\Lambda\frac{\partial f}{\partial\sigma'_{ij}} \tag{16}$$

where the proportionality constant Λ can be determined from the consistency condition.

Differentiating Eq. (15) leads to

$$\mathrm{d}f=\frac{\partial f}{\partial\sigma'_{ij}}\mathrm{d}\sigma'_{ij}+\frac{\partial f}{\partial p'_0}\mathrm{d}p'_0+\frac{\partial f}{\partial p'_{\mathrm{s}}}\mathrm{d}p'_{\mathrm{s}} \tag{17}$$

Differentiating Eq. (14), we have

$$\mathrm{d}p'_0=\frac{\partial p'_0}{\partial p_0'^*}\mathrm{d}p_0'^*+\frac{\partial p'_0}{\partial s}\mathrm{d}s \tag{18}$$

where

$$\frac{\partial p'_0}{\partial p_0'^*}=\frac{\lambda(0)-\kappa}{\lambda(s)-\kappa}\left(\frac{p_0'^*}{p'_n}\right)^{\frac{\lambda(0)-\lambda(s)}{\lambda(s)-\kappa}}\left(s+p_0'^*\right)^{\frac{\kappa_{\mathrm{vs}}}{\lambda(s)-\kappa}}+\frac{\kappa_{\mathrm{vp}}p'_n\left(s+p_0'^*\right)^{\frac{\kappa_{\mathrm{vs}}-\lambda(s)+\kappa}{\lambda(s)-\kappa}}}{\left(\lambda(s)-\kappa\right)\left(s+1\right)}\left(\frac{p_0'^*}{p'_n}\right)^{\frac{\lambda(0)-\kappa}{\lambda(s)-\kappa}} \tag{19}$$

$$\frac{\partial p'_0}{\partial s}=\frac{\kappa_{\mathrm{vs}}p'_0}{\lambda(s)-\kappa}\left[\frac{1}{s+p_0'^*}-\frac{\ln(s+p_0'^*)}{s+1}-\frac{\lambda_{\mathrm{s}}p_{\mathrm{at}}}{\kappa_{\mathrm{vs}}(p_{\mathrm{at}}+s)^2}\ln\left(\frac{p'_0}{p'_n}\right)\right] \tag{20}$$

Substituting Eq. (18) into Eq. (17) gives

$$\mathrm{d}f=\frac{\partial f}{\partial\sigma'_{ij}}\mathrm{d}\sigma'_{ij}+\frac{\partial f}{\partial p'_0}\frac{\partial p'_0}{\partial p_0'^*}\mathrm{d}p_0'^*+\left(\frac{\partial f}{\partial p'_0}\frac{\partial p'_0}{\partial s}+\frac{\partial f}{\partial p'_{\mathrm{s}}}\frac{\partial p'_{\mathrm{s}}}{\partial s}\right)\mathrm{d}s \tag{21}$$

When the stress state is on the LC yield curve, the plastic volumetric strain increment is given by

$$\mathrm{d}\varepsilon_{\mathrm{v}}^{\mathrm{p}}=\frac{(\lambda(0)-\kappa)\mathrm{d}p_0'^*}{(1+e)p_0'^*} \tag{22}$$

On the same yield surface, the plastic volumetric strain increment $\mathrm{d}\varepsilon_{\mathrm{v}}^{\mathrm{p}}$ induced in the saturated soil by $\mathrm{d}p_0'^*$ is the same as the one induced in the unsaturated soil by both $\mathrm{d}p'_0$ and $\mathrm{d}s$. The combination of Eq. (22) with Eq. (16) leads to

$$\mathrm{d}p_0'^*=\frac{(1+e)p_0'^*}{(\lambda(0)-\kappa)}\Lambda\frac{\partial f}{\partial p'} \tag{23}$$

Substituting Eq. (23) into Eq. (21) and taking into account the constitutive model of unsaturated soils, the proportionality constant Λ is obtained:

$$\Lambda=\left[\left(\frac{\partial f}{\partial\sigma'_{ij}}\right)^{\mathrm{T}}\boldsymbol{D}^{\mathrm{e}}\mathrm{d}\varepsilon_{ij}+\left(\frac{\partial f}{\partial p'_0}\frac{\partial p'_0}{\partial s}+\frac{\partial f}{\partial p'_{\mathrm{s}}}\frac{\partial p'_{\mathrm{s}}}{\partial s}+\right.\right.$$

$$\left(\frac{\partial f}{\partial \sigma'_{ij}}\right)^{\mathrm{T}} \boldsymbol{W}^{\mathrm{e}} \mathrm{d}s\Bigg)\Bigg] \Bigg/ \Bigg[\left(\frac{\partial f}{\partial \sigma'_{ij}}\right)^{\mathrm{T}} \boldsymbol{D}^{\mathrm{e}} \frac{\partial f}{\partial \sigma'_{ij}} -$$

$$\frac{\partial f}{\partial p'_0} \frac{\partial p'}{\partial p'^{*}_0} \frac{(1+e)p'^{*}_0}{(\lambda(0)-\kappa)} \frac{\partial f}{\partial p'}\Bigg] \tag{24}$$

where $\boldsymbol{D}^{\mathrm{e}}$ is the elastic stress−strain stiffness matrix and $\boldsymbol{W}^{\mathrm{e}}$ is the elastic suction−strain vector. Therefore, it is possible to calculate the plastic strain increments caused both by the increase in the average skeleton stress and the decrease in suction.

6 Validation of modified BBM

In this section, the results of triaxial tests on unsaturated compacted Pearl clay performed by SUN et al [18] simulated using the modified BBM as well as the BBM to validate the proposed model. The model parameters from Ref. [18] are listed in Table 1.

Table 1 Model parameters

M	$\lambda(0)$	κ	λ_{s}	p'_0/kPa	p'_n/MPa	e_i	κ_{vp}
1.05	0.2	0.03	0.15	100	1.65	1.11	0.0015

Figures 3 and 4 show the comparison of the measured and predicted stress−strain relations of the triaxial tests under a constant mean net stress p=196 kPa, plotted in terms of the principal stress ratio σ_1/σ_3, the principal strains (ε_1 and ε_3), and the volumetric strain ε_{v}. In Fig. 3, suction remains a constant value of 147 kPa during shearing; in Fig. 4, suction decreases from 147 kPa to 0 kPa at different stress ratios during shearing. It can be seen that the predicted stress−strain relations by the BBM and the modified BBM are the same in triaxial compression. The modified BBM predicts the experimental data better than the BBM for the wetting

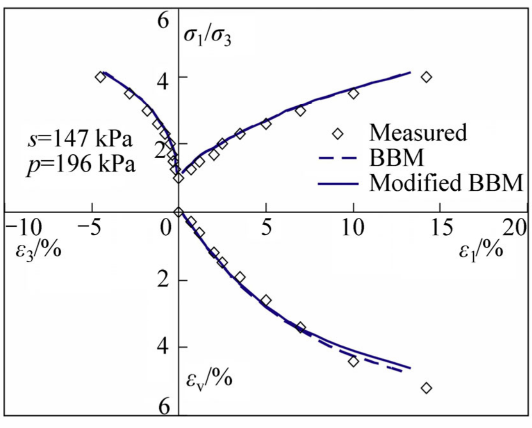

Fig. 3 Predicted and measured stress−strain relations under a constant suction and a constant mean net stress

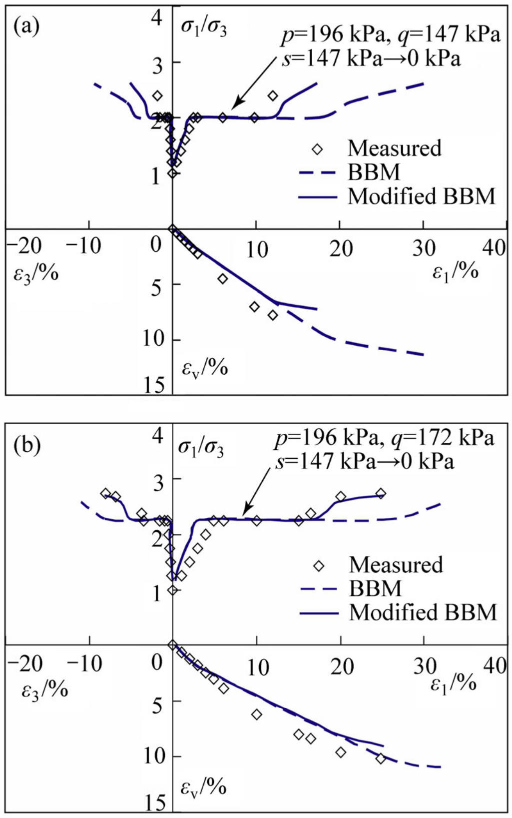

Fig. 4 Predicted and measured stress−strain relations with suction decreasing from 147 kPa to 0 at different stress ratios during shearing: (a) Collapsing at σ_1/σ_3=2; (b) Collapsing at σ_1/σ_3=2.5

deformation, which illustrates the reasonability of the modified BBM to predict the collapse behavior of unsaturated soils. Besides, it is noted from Fig. 4 that both the axial and the lateral strain increments induced by collapse are greater at a high stress ratio than at a low stress ratio, while the volumetric strain increment is almost the same at different stress ratios. This phenomenon means that the volumetric collapsing strain is mainly dependent on the mean net stress, while the shear collapsing strain is dependent on the stress ratio.

7 Numerical analysis of a model slope

The failure of a slope is often induced by rainfall infiltration because of the change of the pore-water pressure and the stress and strain in soil. To demonstrate this mechanism of the slope failure, the finite element analysis incorporated with the modified BBM was carried out on a homogenous model slope.

An idealized homogeneous slope with a height of 10 m and a gradient of 1:1.5 is analyzed in this work. As shown in Fig. 5, a large length of 55 m in the numerical modelling is selected to reduce the influence of the boundaries in both left and right sides. The initial ground water level is assumed to be horizontal and at the height of points F and E. The boundary conditions include seepage boundary and displacement boundary. The seepage boundary is prescribed as follows: the bottom of the mesh $\overline{AB}$ is assumed to be impermeable, whereas the ground surfaces $\overline{CD}$, $\overline{DE}$ and $\overline{EF}$ are flux boundaries receiving rainwater infiltration. Lateral surfaces $\overline{BC}$ and $\overline{AF}$ are set as zero-flux boundaries and any seepage face is calculated automatically by the FEM program. For the displacement boundary, $\overline{BC}$ and $\overline{AF}$ at the right and left sides are set to be zero in horizontal displacements, and $\overline{AB}$ at the bottom is fixed.

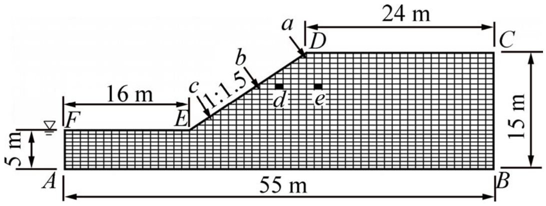

Fig. 5 Model slope and finite element mesh

Due to the variation of the infiltration capacity with time, it is difficult to determine the flux boundary in the process of rainfall infiltration. When the rainfall intensity is less than the soil infiltration capacity, all the rainfall can percolate into the soil. However, when the rainfall intensity is larger than the soil infiltration capacity, the part of the rainfall larger than the soil infiltration capacity forms the surface flow, and does not influence the water pressure in slope under rainfall. Therefore, to model the infiltration process of rainfall, the flux at the slope surface is controlled. When the rainfall intensity is greater than the infiltration capacity, a constant water pressure (u_w=0) is prescribed on all the nodes at the slope surface. However, the infiltration capacity cannot be determined before the distribution of water pressure is obtained at each calculation step. In this case, an iterative procedure is required to determine the exact flux boundary conditions. In this analysis, the rainfall is supposed with an intensity of 10 mm/h (2.8×10^{-6} m/s) during 10 days (240 h), and thus the total rainfall is 2400 mm.

The parameters used include the mechanical parameters involved in the modified BBM which are listed in Table 1 and the hydraulic parameters of the soil−water characteristic curve. A widely used representation of the hydraulic characteristic of unsaturated soils is the set of closed-form equations formulated by van GENUCHTEN, which is based on the capillary model of MUALEM. The soil−water characteristic curve and the permeability functions are given by

$$S_r = (S_{sw} - S_{rw})\left[1 + \left(s/p_0\right)^n\right]^{-m} + S_{rw} \tag{25}$$

$$k_r = S_e^{1/2}\left[1 - \left(1 - S_e^{1/m}\right)^m\right]^2 \tag{26}$$

$$S_e + (S_r - S_{rw})/(S_{sw} - S_{rw}) \tag{27}$$

where p_0 is the air entry potential, n and m are the parameters which satisfy the relation m=1−1/n. k_r is the relative coefficient of permeability. S_e is the effective degree of saturation. S_{rw} is the residual degree of saturation. S_{sw} is the maximum degree of saturation.

The parameters of the van GENUCHTEN hydraulic characteristic in this analysis are cited from Ref. [19] as follows: p_0=10.6 kPa, n=1.395, S_{rw}=0.28, S_{sw}=1.0, k_{sw}=1.516×10^{-6} m/s. The soil−water characteristic curve and the relative permeability used in the analysis are shown in Fig. 6.

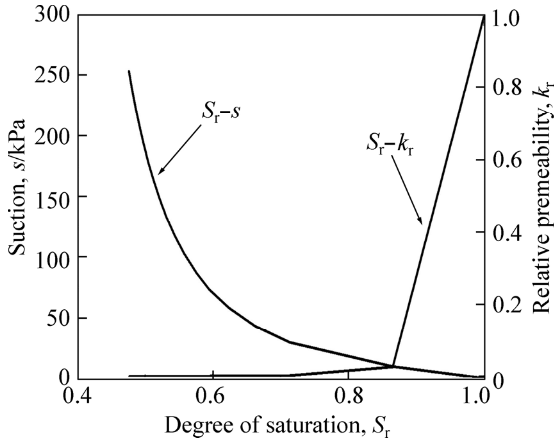

Fig. 6 Hydraulic characteristics

In this work, the initial degree of saturation, S_r, is assumed to be 78.9% at the crest of the slope, and linearly increases with depth to 100% at the level of the groundwater table. Consequently, the initial pore-water pressure can be computed by substituting the initial degree of saturation into Eq. (25). Besides, since the soil behavior is a function of the stress state for nonlinear elasto-plastic models, it is necessary to estimate the initial in situ stress state prior to the beginning of infiltration. To establish in situ stress that satisfies the equilibrium equation, body forces are merely turned on with gravity, and in this work, the type of stress history of the slope is not taken into account. Finally, the initial stress is obtained by simulating the stage construction until the slope is raised up to the height of 10 m.

To illustrate the results of numerical analysis, five elements in Fig. 5 are selected. Elements a−c are in the slope surface with different heights, while elements d and e are in deeper positions which are at the same level as element b. Figure 7 presents the time history of pore-water pressure at elements a−e. Figure 8 shows the contours of the pore-water pressure in the slope at several different moments after rainfall. It is seen that the

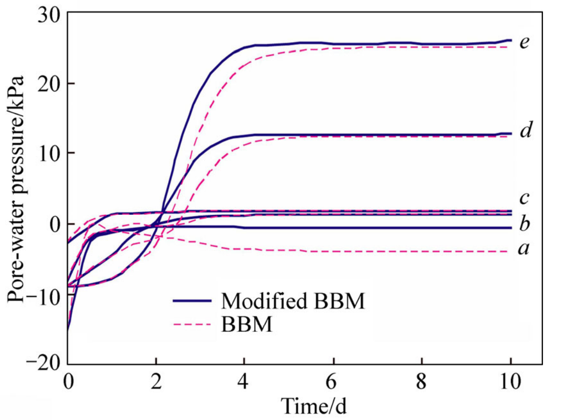

Fig. 7 Time history of pore-water pressure at selected elements

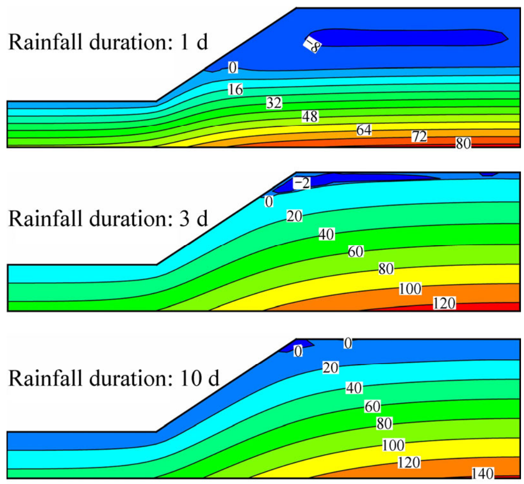

Fig. 8 Contours of pore water pressure (Unit: kPa)

elements a–c near the slope surface have relatively higher initial negative pore-water pressure, which increases quickly after rainfall and converges to zero. On the contrary, the pore-water pressure in the elements d and e in deeper positions increases slowly at the beginning of rainfall and increases suddenly after rainfall continues over 2 days. This is because there exists an unsaturated zone above the groundwater level, where the permeability is comparatively low. The elements near the slope surface tend to be saturated quickly due to the rainfall. The unsaturated zone inside the slope becomes smaller and smaller with the infiltration of rainfall from both the crest of the slope and the slope surface. When the unsaturated zone disappears, the groundwater level suddenly rises in the slope since the saturated permeability (1.516×10^{-6} m/s) is less than the rainfall intensity (2.8×10^{-6} m/s) and the infiltrated rainwater cannot be easily drained. Thus, the failure of a slope under rainfall infiltration is due to both the reduction of soil suction and the significant rise in groundwater table. It can be also found that the predicted pore-water pressure by the modified BBM increases more quickly than that by the BBM when the soil is fully saturated. This may be due to the replacement of the net stress by the average skeleton stress in the modified BBM, and the deformation of the soil can contribute to the change of the pore-water pressure partly.

Figure 9 shows the calculated contours of the horizontal and vertical displacements at different moments after rainfall. It is seen from Fig. 9(a) that the negative horizontal displacements (outwards the slope) are generated in the zone where infiltrated rainwater has reached the surface, resulting from the reduction of soil suction and thereby the decrease in the shear strength of soil. In accordance with some experimental observation [20−21], the horizontal displacement calculated in this work increases from the inner to the outer side of the slope and its maximum value appears in upper area of the slope surface where the soil slide is likely to take place. As seen in Fig. 9(b), both negative displacement (settlement) and positive vertical displacement (heave) are generated in the slope during the infiltration of rainfall. The settlement, equivalent to the wetting-induced collapse deformation, takes place in the shallow

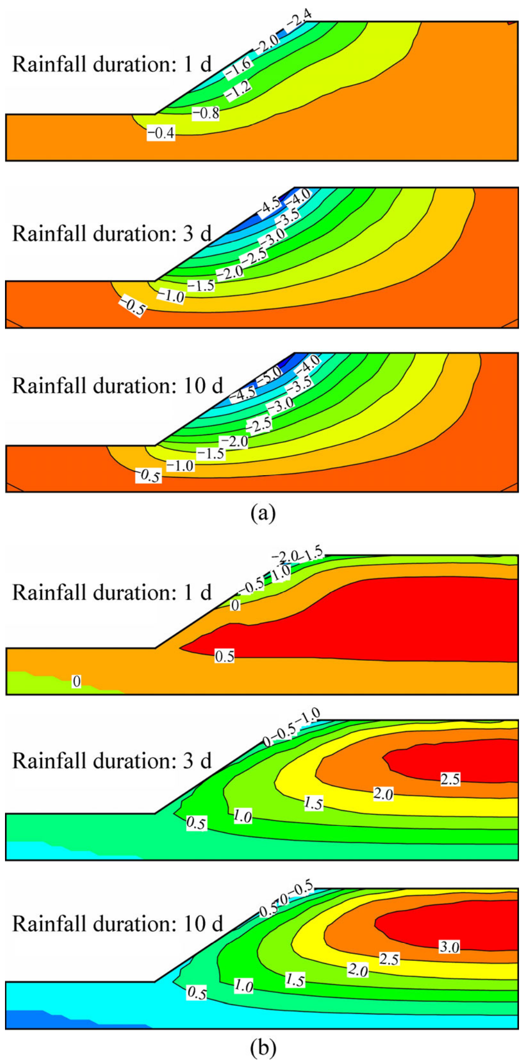

Fig. 9 Contours of displacements (cm): (a) Horizontal displacement; (b) Vertical displacement

depth of the slope surface as a result of the reduction of soil suction. The heave, resulting from the increase in soil pore-water pressure and the decrease in effective stress, happens inside the slope and continuously increases with the rise of groundwater level. Figure 10 presents the displacement vectors after the rainfall lasts for three days, which is similar to the observation from the model test [21].

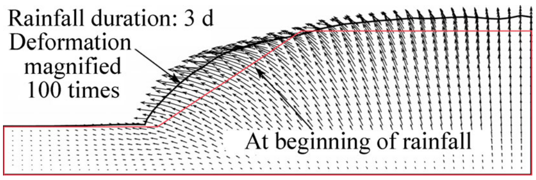

Fig. 10 Distribution of displacement vectors

Figure 11 shows the evolution of the displacements at the centers of the selected elements during the infiltration of rainfall. It is noted that the evolution of the displacements is greatly related to the change of pore-water pressure. As shown in Fig. 7, there is a critical moment when the pore water pressure increases suddenly from a negative value to a positive value. Before the critical moment, the soil is in an unsaturated state and the decrease of suction caused by the infiltration of rainfall results in a relatively fast evolution

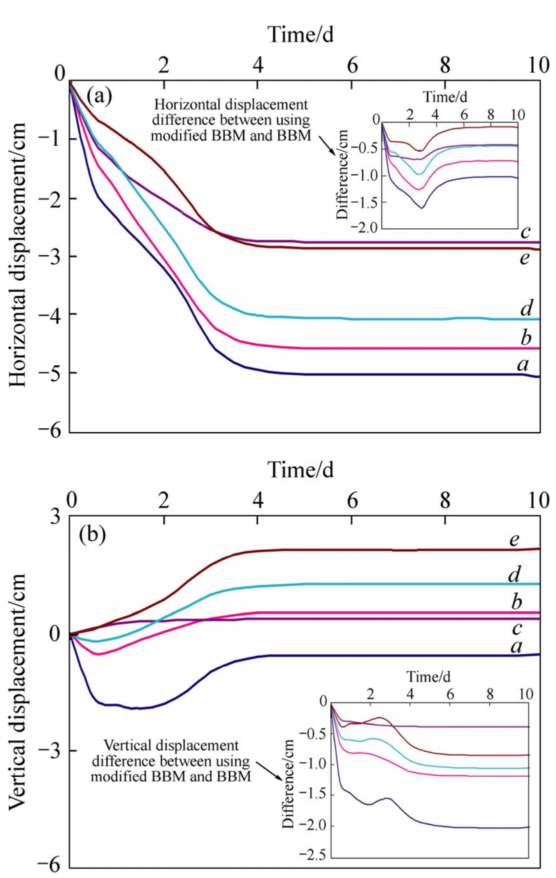

Fig.11 Time history of displacements at selected nodes: (a) Horizontal displacement; (b) Vertical displacement

of the displacements (i.e. wetting-induced collapse). After the critical moment, the soil becomes saturated and the continuity of the infiltration of rainfall causes the increase of the pore-water pressure and the decrease of the effective stress. Consequently, the soil rebounds and the displacements at the selected nodes decrease, especially at the nodes *a*−*c* near the slope surface. The difference of the displacement between using modified BBM and BBM is also given in Fig. 11. It is noted that the predicted displacement by the modified BBM is smaller. For the horizontal displacement, the maximum difference occurs when the rainfall lasts for three days. While the vertical displacement difference increases except at the second day of the rainfall. As mentioned, the normal compression lines at different suctions diverge and converge with increasing applied stress for BBM and modified BBM, respectively. Thus, the wetting deformation predicted by the modified BBM can be reduced. Besides, the inflection point on the displacement difference−time curve can be explained by the existence of a discontinuity at the transition from saturated to unsaturated states for BBM.

The slope stability analysis for this case study is performed by utilizing the limiting equilibrium-based program, in which the pore-water pressure is obtained from the forgoing coupled analysis. The slope stability increases when the shear strength contributed by the matric suction is taken into account. The shear strength is calculated using two different friction angles, which is adopted by FREDLUND et al [22]. An additional friction angle Φ^b is assumed to be related to the matric suction. In this analysis, S_r is assumed to be ($\tan\Phi^b/\tan\Phi'$), and the mechanical parameters are given as follows: effective cohesion c'=8 kPa, effective friction angle Φ'=30°, and unit weight γ=18 kN/m^3. The time history of the safety factor of model slope is shown in Fig. 12. It is indicated that the slope failure takes place during the rainfall with intensity of 10 mm/h after about two days, when the safety factor states to be less than 1.0. By comparing the slope stability results to the infiltration analysis results

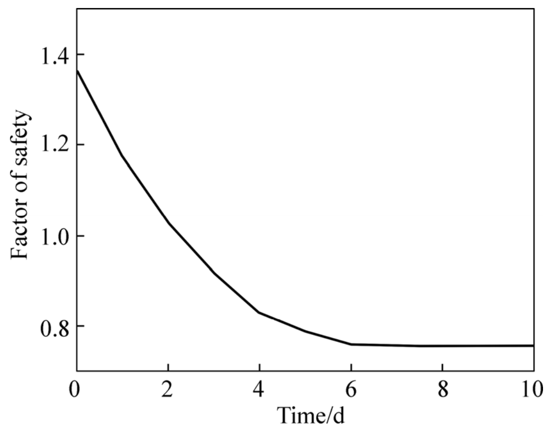

Fig. 12 Time history of safety factor of model slope

in Fig. 7, it is seen that the stability changes first in response to a decrease in matric suction up to approximately two days, then in response to an increase of positive pore water pressures in the slope. After six days of rainfall, the safety factor of slope reaches the minimum value of 0.76 and varies slightly while the rainfall infiltration continues.

8 Conclusions

1) The convergence of the normal compression lines at different values of suction in the range of larger isotropic stress is satisfied in the modified BBM.

2) Replacing the net stress with the average stress can simplify the constitutive modeling for unsaturated soils and the discontinuity at the transition from saturated to unsaturated states is avoided.

3) The collapse deformation of unsaturated soils can be well predicted by the modified BBM for the unsaturated soils where the normal compression lines at different values of suction converge with increasing applied stress.

4) The reasonable distributions of the pore-water pressure and the displacements in a model slope under the infiltration of rainfall are obtained simultaneously by using the modified BBM.

5) The reduction of the slope stability is mainly attributed to the decrease in shear strength caused by the loss of suction from the unsaturated to saturated state and the reduction of effective stress for groundwater level rising significantly due to the low permeability.

References

[1] COLLINS B D, ZNIDARCIC D. Stability analyses of rainfall induced landslides [J]. Journal of Geotechnical and Geoenvironmental Engineering, 2004, 130(4): 362−372.

[2] CHO S E, LEE S R. Instability of unsaturated soil slopes due to infiltration [J]. Computers and Geotechnics, 2001, 28(3): 185−208.

[3] SHENG D, SMITH D W, SLOAN S W, GENS A. Finite element formulation and algorithms for unsaturated soils. Part II: Verification and application [J]. International Journal for Numerical and Analytical Methods in Geomechanics, 2003, 27: 767−790.

[4] GARCIA E, OKA F, KIMOTO S. Instability analysis and simulation of water infiltration into an unsaturated elasto-viscoplastic material [J]. International Journal of Solids and Structures, 2010, 47: 3519−3536.

[5] ALONSO E E, GENS A, DELAHAYE C H. Influence of rainfall on the deformation and stability of a slope in overconsolidated clays: A case study [J]. Hydrogeol, 2003, 11: 174−192.

[6] FAN Zhen-hui, ZHANG Chun-shun, XIAO Hong-bin. Simulation analysis of deformation for unsaturated expansive soils based on fluid-solid coupling characteristics [J]. Journal of Central South University (Science and Technology), 2011, 42(3): 758−764. (in Chinese)

[7] ALONSO E E, GENS A, JOSA A A. Constitutive model for partially saturated soils [J]. Géotechnique, 1990, 40(3): 405−430.

[8] WHEELER S J, SIVAKUMAR V. An elasto-plastic critical state framework for unsaturated soil [J]. Géotechnique, 1995, 45: 35−53.

[9] LORET B, KHALILI N. An effective stress elastic-plastic model for unsaturated porous media [J]. Mechanics of Materials, 2002, 34: 97−116.

[10] GENS A, SANCHEZ M, SHENG D. One constitutive modeling of unsaturated soils [J]. Acta Geotechnica, 2006, 1(3): 137−147.

[11] GALLIPOLI D, GENS A, SHARMA R, VAUNAT J. An elastoplastic model for unsaturated soil incorporating the effects of suction and degree of saturation on mechanical behaviour [J]. Géotechnique, 2003, 53(1): 123−135.

[12] MEI Guo-xiong, CHEN Qi-ming, JIANG Peng-ming. Stress-strain relationship of unsaturated cohesive soil [J]. Journal of Central South University of Technology, 2010, 17(3): 653−657.

[13] SUN D A, SHENG D, LI X, SLOAN S W. Elastoplastic modelling of hydraulic and stress-strain behaviour of unsaturated soils under undrained conditions [J]. Computers and Geotechnics, 2008, 35: 845−852.

[14] ZHOU A N, SHENG D, SLOSN S W, GENS A. Interpretation of unsaturated soil behaviour in the stress–Saturation space. I: Volume change and water retention behaviour [J]. Computers and Geotechnics, 2012, 43: 178−187.

[15] SHENG D, GENS A, FREDLUND D G, SLOAN S W. Unsaturated soils: From constitutive modeling to numerical algorithms [J]. Computers and Geotechnics, 2008, 35: 810−824.

[16] YUDHBIR. Collapsing behaviour of residual soils [C]// Proc 7th SE Asian Geotech Conf. Hong Kong: Institute of Engineers, 1982: 915−930.

[17] JOSA A, BALMACEDA A, GENS A. An elasto-plastic model for partially saturated soils exhibiting a maximum of collapse [C]// Processing 3rd International Conference on Computational Plasticity. Barcelona: 1992: 815−826.

[18] SUN A, MATSUOKA H, YAO P, ICHIHARA W. An elasto-plastic model for unsaturated soil in three dimensional stresses [J]. Soils and Foundations, 2000, 40(3): 17−28.

[19] CAI F, UGAI K. Numerical analysis of rainfall effects on slope stability [J]. International Journal of Geomechanics, 2004, 4(2): 69−78.

[20] CHEN R H, CHEN H P, CHEN K S, ZHUNG H B. Simulation of a slope failure induced by rainfall infiltration [J]. Environmental Geology, 2009, 58: 943−952.

[21] QIAN Ji-yun, ZHANG Ga, ZHANG Jian-min, LEE C F. Centrifuge model tests of cohesive soil slopes during rainfall [J]. J Tsinghua Univ (Sci & Tech), 2009, 49(6): 813−817. (in Chinese)

[22] FREDLUND D G, MORGENSTERN N R, WIDGER R A. The shear strength of unsaturated soils [J]. Journal of Canadian Geotechnical, 1978, 15: 313−321.

(Edited by YANG Bing)